

## Electrochemical Adsorption Properties and Inhibition of Zinc Corrosion by Two Chromones in Sulfuric Acid Solutions

Abd El-Aziz S. Fouda\*, Ahmed Abdel Nazeer†, and Ahmed Saber

Department of Chemistry, Faculty of Science, El-Mansoura University, El-Mansoura-35516, Egypt.

\*E-mail: [asfouda@mans.edu.eg](mailto:asfouda@mans.edu.eg)

†Electrochemistry and Corrosion Lab., National Research Centre, Dokki, Cairo-12622, Egypt

(Received October 23, 2013; Accepted March 4, 2014)

**ABSTRACT.** The electrochemical behavior and corrosion inhibition of zinc in 0.5 M H<sub>2</sub>SO<sub>4</sub> in the absence and presence of some chromones has been investigated using weight loss, potentiodynamic polarization, electrochemical impedance spectroscopy (EIS) and electrochemical frequency modulation (EFM) techniques. The presence of these investigated compounds in the corrosive solutions decrease the weight loss, the corrosion current density, and double layer capacitance but increases the charge transfer resistance. Polarization studies were carried out at room temperature, and showed that all the studied compounds act as mixed type inhibitors with a slight predominance of cathodic character. The effect of temperature on corrosion inhibition has been studied and the thermodynamic activation and adsorption parameters were determined and discussed. The adsorption of the investigated compounds on zinc was found to obey Langmuir adsorption isotherm.

**Key words:** Corrosion inhibition, Zinc, H<sub>2</sub>SO<sub>4</sub>, EIS, EFM

### INTRODUCTION

Zinc is widely used in various industrial operations and the study of corrosion of zinc and its inhibition is a subject of practical significance. The damage by corrosion generates high cost for inspection, repairing, and replacement, thus the necessity of using substances that behave like corrosion inhibitors especially in acid media<sup>1</sup> is required. The use of organic molecules as corrosion inhibitor is one of the most practical methods for protecting against the corrosion, and it is becoming increasingly popular. Organic inhibitors act by the adsorption and forming protective film on the metal surface. Organic compounds containing heteroatoms with high electron density, such as N, P, S, and O in their molecular structures as well as those containing multiple bonds are effective as corrosion inhibitor because of their ability to be adsorbed on the metal surface.<sup>2–5</sup> Many researchers in the literature studied the corrosion inhibition of zinc in H<sub>2</sub>SO<sub>4</sub> using organic compounds containing nitrogen, oxygen and/or sulphur atoms. Among nitrogen containing compounds: quinoline,<sup>6</sup> aniline,<sup>7</sup> hydrazine derivatives,<sup>8</sup> tetrahydrocarbazole derivatives,<sup>9</sup> thiourea,<sup>10</sup> benzene-thiol and its derivatives,<sup>11</sup> imidazole azo derivatives,<sup>12</sup> 2-mercaptopbenzimidazole,<sup>13</sup> Schiff bases of ethylenediamine<sup>14</sup> and *m*-substituted aniline-*N*-salicylidene<sup>15</sup> these compounds have shown good inhibition towards zinc in acidic medium. On other hand, quinine sulphate, pip-

erazine, caffeine and barbitone have been investigated as corrosion inhibitors for aluminum and zinc in acidic medium.<sup>16,17</sup> The reaction of corrosion inhibitors at the metal-solution interface has been evaluated by adsorption characteristics and also by the thermodynamics of adsorption.<sup>18,19</sup>

The aim of the present work deals with the effect of two chromone derivatives on the corrosion of zinc in H<sub>2</sub>SO<sub>4</sub> solution using weight loss and different electrochemical measurements. The effect of temperature on corrosion behavior also was studied and the mechanism of corrosion inhibition was discussed. Activation energies in the absence and presence of inhibitors have been evaluated.

### EXPERIMENTAL

The zinc (BDH grade) sheets used in this paper have the following composition (weight %): 0.003 Cu, 0.002 Fe, 0.001 Pb, 0.001 Cd and the rest Zn. All chemicals used were of analytical reagent grade. Specimens of zinc sheets were first polished with different grades of emery papers, in order to obtain a smooth surface, then degreased in acetone in ultrasonic bath, washed by bidistilled water and dried between two filter papers. The solution of 0.5 M H<sub>2</sub>SO<sub>4</sub> was prepared with bidistilled water. The names, molecular formulae, structures and molecular weights of the investigated chromones are:

Comp.	Structures	Names	M. Formulae. & Mol. Weights
a		3-hydroxy-6,7,8-trimethoxy-2-phenyl-4H-chromen-4-one	C <sub>18</sub> H <sub>16</sub> O <sub>6</sub> 328.32
b		3-bromo chromone	C <sub>9</sub> H <sub>5</sub> BrO <sub>2</sub> Mol.Wt.: 225.04

### Weight Loss Measurements

For weight loss measurements, rectangular zinc specimens of size 20×20×2 mm were immersed in 100 ml inhibited and uninhibited solutions and allow to stand for several intervals at 30 °C in water thermostat. The degree of surface coverage ( $\theta$ ) and the percentage inhibition efficiency (% IE) of the studied inhibitors was calculated using equation (1):

$$\% \text{IE} = \theta \times 100 = [1 - (M_{\text{inh}}/M_{\text{free}})] \times 100 \quad (1)$$

where  $M_{\text{free}}$  and  $M_{\text{inh}}$  are the weight losses per unit area in the absence and presence of the investigated compounds, respectively.

### Potentiodynamic Polarization Measurements

Potentiodynamic polarization experiments were carried out in a conventional three-electrode cell with platinum foil (1 cm<sup>2</sup>) as counter electrode, a saturated calomel electrode (SCE) as a reference electrode and zinc sheet (1×1 cm) embedded in epoxy resin of polytetrafluoroethylene as a working electrode. Before polarization scanning, working electrode was immersed in the test solution for 30 minute until steady state potential was attained. Measurements were performed in the 0.5 M H<sub>2</sub>SO<sub>4</sub> solution containing different concentrations of the investigated compounds by changing the electrode potential automatically from -1.5 to -0.25 V at scan rate of 0.5 mV s<sup>-1</sup>. The linear Tafel segments of anodic and cathodic curves were extrapolated to corrosion potential to obtain corrosion current densities ( $i_{\text{corr}}$ ). The inhibition efficiency (% IE) and the degrees of surface coverage ( $\theta$ ) were defined by equation (2):<sup>20</sup>

$$\% \text{IE} = \theta \times 100 = [1 - (i_{\text{corr}}/i'_{\text{corr}})] \times 100 \quad (2)$$

where  $i_{\text{corr}}$  and  $i'_{\text{corr}}$  are the inhibited and uninhibited corrosion current density values, respectively.

### Electrochemical Frequency Modulation (EFM) Technique

Electrochemical frequency modulation technique is a non destructive technique that can directly and rapidly gives values of the corrosion current without a prior knowledge of Tafel constants. In this work, potential perturbation signal with amplitude of 10 mV with two sine waves of 2 and 5 Hz was applied. The intermodulation spectra containing current responses were assigned for harmonical and intermodulation current peaks. The larger peaks were used to calculate the corrosion current density ( $i_{\text{corr}}$ ), the Tafel constants ( $\beta_c$  and  $\beta_a$ ) and the causality factors CF-2 and CF-3.

### Electrochemical Impedance Spectroscopy (EIS) Method

Electrochemical impedance spectroscopy (EIS) tests were performed at 25 ± 1 °C in a three electrode assembly. The EIS spectra were recorded at open circuit potential (OCP) after immersion the electrode for 30 minutes in the test solution. The AC signal was 5 mV peak to peak and the frequency range studied was between 100 kHz and 0.2 Hz. The inhibition efficiency (% IE) and the surface coverage ( $\theta$ ) of the used inhibitor obtained from the impedance measurements can be calculated from equation (3):

$$\% \text{IE} = \theta \times 100 = [(R_{\text{ct}} - R'_{\text{ct}})/R_{\text{ct}}] \times 100 \quad (3)$$

where  $R'_{\text{ct}}$  and  $R_{\text{ct}}$  are the charge transfer resistance in the presence and absence of inhibitor, respectively.

All electrochemical experiments were carried out using Gamry PCI 300/4 Potentiostat/Galvanostat/Zra analyzer, DC 105 corrosion software, EIS 300 Electrochemical impedance software, EFM 140 Electrochemical frequency modulation software and Echem Analyst 5.21 for results plotting, graphing, data fitting and calculating.

## RESULTS AND DISCUSSION

### Weight Loss Measurements

Weight loss-time curves for the corrosion of zinc in 0.5 M H<sub>2</sub>SO<sub>4</sub> in the absence and presence of different concentrations of the studied chromones at 25 °C were determined as shown in Fig. 1. As shown from this Figure, by increasing the concentration of these compounds, the weight loss of zinc is decreased. The linear variation of weight loss with time in uninhibited and inhibited 0.5 M H<sub>2</sub>SO<sub>4</sub> indicates the absence of insoluble surface films during corrosion. From the calculated values of inhibition efficiency given in Table 1, it is obvious that the inhibition increases by increasing the concentration of the additives. This indi-

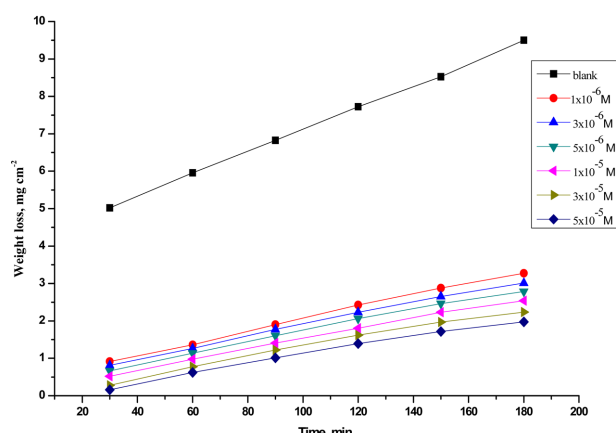


**Figure 1.** Weight loss-time curves for zinc dissolution in 0.5 M  $\text{H}_2\text{SO}_4$  in the absence and presence of different concentration of compound (a) at 25 °C.

**Table 1.** Effect of inhibitors concentrations on the percentage inhibition efficiency (% IE) of zinc in 0.5 M  $\text{H}_2\text{SO}_4$  solution from weight loss method at 25 °C

Conc., M	Inhibition efficiency	
	(a)	(b)
$1 \times 10^{-6}$	68.6	66.7
$3 \times 10^{-6}$	71.1	68.4
$5 \times 10^{-6}$	73.3	70.8
$1 \times 10^{-5}$	76.6	73.4
$3 \times 10^{-5}$	79.2	75.5
$5 \times 10^{-5}$	81.9	78.4

cates that the additives behave as inhibitors over the concentration range studied. The order of decreasing the inhibition efficiency of the investigated derivatives (*Table 1*) in 0.5 M  $\text{H}_2\text{SO}_4$  is: (a) > (b).

### Adsorption isotherm

One of the most convenient ways of expressing adsorption quantitatively is by deriving the adsorption isotherm that characterizes the metal/inhibitor/environment system.<sup>21</sup> Assuming the corrosion inhibition was caused by the adsorption of chromones, the values of surface coverage for different concentrations of inhibitors in 0.5 M  $\text{H}_2\text{SO}_4$  were evaluated from weight loss measurement using equation (1). It was found that the values of ( $\theta$ ) increased with increasing the concentration of chromones. Using these values

**Table 2.** Equilibrium constant ( $K_{ads}$ ) and free energy of binding  $\Delta G^o_{ads}$ , for chromone derivatives at 25 °C

Inhibitors	Langmuir adsorption isotherm			
	$K_{ads} \times 10^5 \text{ M}^{-1}$	$-\Delta G^o_{ads}, \text{ kJ mol}^{-1}$	slope	$R^2$
(a)	7.8864	43.6	1.141	0.9997
(b)	4.0032	41.9	1.235	0.9998

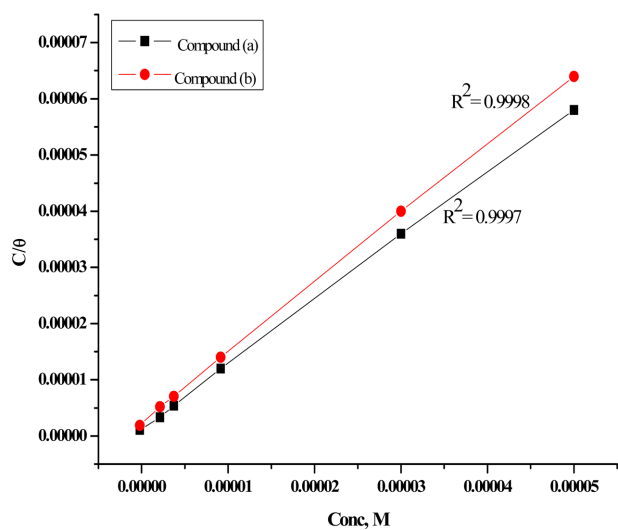


**Figure 2.** Langmuir adsorption isotherm plots for zinc in 0.5 M  $\text{H}_2\text{SO}_4$  containing various concentrations of compounds (a and b) at 25 °C.

of surface coverage, one can utilize different adsorption isotherms to deal with experimental data.

Different adsorption isotherms were applied to investigate the adsorption mechanism and the best one obtained is Langmuir isotherm by plotting  $(C/\theta)$  vs  $C$ , straight lines were obtained (*Fig. 2*) indicating that this isotherm is valid for these compounds. Langmuir adsorption isotherm<sup>22</sup> expressed by equation (4):

$$C/\theta = 1/K_{ads} + C \quad (4)$$

where  $C$  is inhibitor concentration and  $K_{ads}$  is equilibrium constant of adsorption. It is well known that the standard adsorption free energy ( $\Delta G^o_{ads}$ ) is related to equilibrium constant of adsorption ( $K_{ads}$ ) by the equation (5):<sup>23</sup>

$$K_{ads} = 1/55.5 \exp(-\Delta G^o_{ads}/RT) \quad (5)$$

where 55.5 is the concentration of water in the bulk of the solution in  $\text{mol L}^{-1}$ ,  $R$  is the universal gas constant and  $T$  is the absolute temperature. The values of  $\Delta G^o_{ads}$  are negative indicating that the adsorption process proceeds spontaneously and the adsorbed layer on the zinc surface is stable.<sup>24</sup> It is generally accepted that the values of  $\Delta G^o_{ads}$  up to  $-20 \text{ kJ mol}^{-1}$  the type of adsorption was regarded as physisorption, the inhibition acts due to the electrostatic interaction between the charged molecules and the charged metal, while the values around  $-40 \text{ kJ mol}^{-1}$  or higher, were seen as chemisorptions, which is due to the charge sharing or a transfer from the inhibitor molecules to the metal surface to form covalent bond.<sup>25,26</sup> The calculated values of  $\Delta G^o_{ads}$  for compounds (a) and (b) are equal to  $-43.6$  and  $-41.9 \text{ kJ}$

$\text{mol}^{-1}$ , respectively. It suggested that the adsorption mechanism of investigated inhibitors on Zn in 0.5 M  $\text{H}_2\text{SO}_4$  solution involves two types of interaction, physisorption and chemisorption.<sup>27,28</sup>

### Effect of temperature

The effect of temperature on the corrosion rate of zinc in 0.5 M  $\text{H}_2\text{SO}_4$  solution in the absence and presence of different concentrations of the investigated chromones was studied at different temperatures (25–55 °C) using weight-loss measurements to calculate the activation parameters of the corrosion process and investigate the mechanism of inhibition.

The activation parameters  $E_a^*$ ,  $\Delta H^*$  and  $\Delta S^*$  are calculated from Arrhenius plot (Eq. 6) and transition state-type equation (Eq. 7):<sup>29</sup>

$$k = A \exp(-E_a^*/RT) \quad (6)$$

$$k = RT/Nh \exp(\Delta S^*/R) \exp(-\Delta H^*/RT) \quad (7)$$

where  $k$  is the corrosion rate of metal,  $A$  is the pre-exponential factor,  $E_a^*$  is the apparent activation energy of the corrosion process,  $\Delta H^*$  is the activation enthalpy and  $\Delta S^*$  is the activation entropy.

Fig. 3 represents plot of  $\log k$  versus  $(1/T)$  for zinc in 0.5 M  $\text{H}_2\text{SO}_4$  solution in the absence and presence of different concentrations of the investigated inhibitors. Straight lines were obtained with slope equal to  $-E_a^*/2.303R$ . The activation energy value obtained 13.5 kJ mol $^{-1}$  for 0.5 M  $\text{H}_2\text{SO}_4$  and increased to 33.0 kJ mol $^{-1}$  in the presence of  $5 \times 10^{-5}$  M of

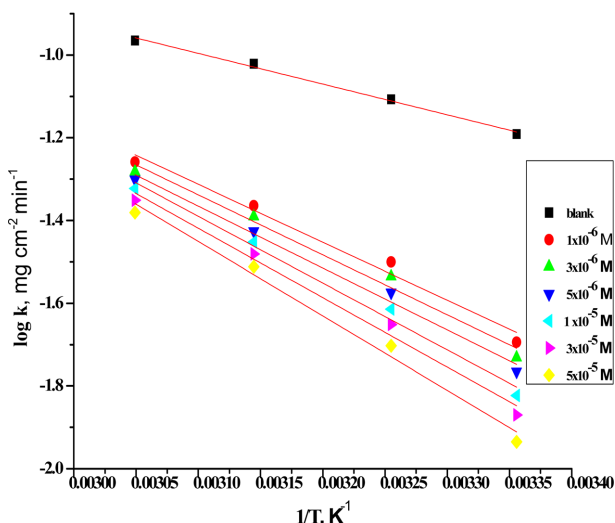


Figure 3. Arrhenius plots ( $\log k$  vs.  $1/T$ ) for zinc in 0.5 M  $\text{H}_2\text{SO}_4$  in the absence and presence of different concentrations of compound (a).

Table 3. Activation parameters for the dissolution of zinc in the absence and presence of different concentrations of chromones in 0.5 M  $\text{H}_2\text{SO}_4$

Inhibitor	Conc., M	Activation parameters		
		$E_a^*$ kJ mol $^{-1}$	$\Delta H^*$ kJ mol $^{-1}$	$-\Delta S^*$ J mol $^{-1}$ K $^{-1}$
Free Acid (0.5 M $\text{H}_2\text{SO}_4$ )	0	13.5	10.9	96.8
(a)	$1 \times 10^{-6}$	25.6	23.0	65.3
	$3 \times 10^{-6}$	27.0	24.4	61.6
	$5 \times 10^{-6}$	27.4	24.8	60.6
	$1 \times 10^{-5}$	29.5	26.9	54.5
	$3 \times 10^{-5}$	30.7	28.1	51.3
	$5 \times 10^{-5}$	33.0	30.5	44.7
(b)	$1 \times 10^{-6}$	24.8	22.2	67.8
	$3 \times 10^{-6}$	24.9	22.3	67.7
	$5 \times 10^{-6}$	25.9	23.3	65.1
	$1 \times 10^{-5}$	27.0	24.4	62.2
	$3 \times 10^{-5}$	27.3	24.7	61.7
	$5 \times 10^{-5}$	28.6	26.0	58.2

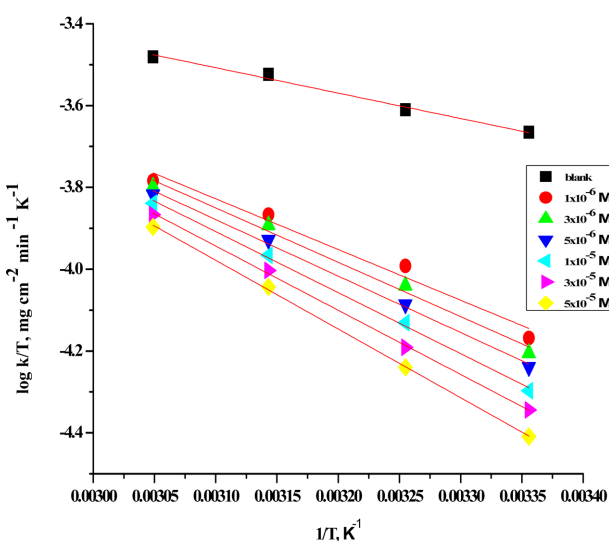
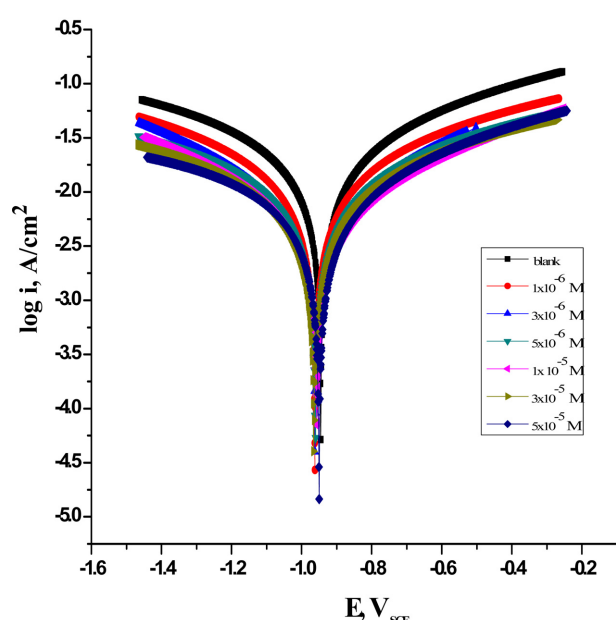


Figure 4. Arrhenius plots ( $\log k/T$  vs.  $1/T$ ) for zinc dissolution in 0.5 M  $\text{H}_2\text{SO}_4$  in the absence and presence of different concentrations of compound (a).

compound (a) and 28.6 kJ mol $^{-1}$  in the presence of  $5 \times 10^{-5}$  M of compound (b) (Table 3). These values show that the presence of the additives increases the activation energy indicating a strong adsorption of the inhibitor molecules on zinc surface and the energy barrier caused by the adsorption of the additive molecules on zinc surface.

Plots of  $\log(k/T)$  vs  $1/T$  are shown in Fig. 4. As shown from this Figure, straight lines with slope of  $(-\Delta H^*/2.303R)$  and intercept of  $(\log(RNh) + \Delta S^*/2.303R)$ . The increase



**Figure 5.** Potentiodynamic polarization curves for corrosion of zinc in 0.5 M  $\text{H}_2\text{SO}_4$  in the absence and presence of different concentrations of compound (a) at 25 °C.

in the activation enthalpy ( $\Delta H^*$ ) in the presence of the inhibitors implies that the addition of the inhibitors to the acid solution increases the height of the energy barrier of the corrosion reaction to an extent depends on the type and concentration of the present inhibitor. The entropy of activation ( $\Delta S^*$ ) in the blank and inhibited solutions is large and negative indicating that the activated complex represents association rather than dissociation step.<sup>30</sup>

#### Potentiodynamic Polarization Measurements

Fig. 5 shows the potentiodynamic polarization curves ( $E$  vs

$\log i$ ) of zinc dissolution in 0.5 M  $\text{H}_2\text{SO}_4$  in the absence and presence of different concentrations of compound (a). Similar curves were obtained in presence of compound (b) (not shown). From this Figure, it is clearly seen that the presence of compound (a) shifts both the anodic and cathodic branches of the polarization curves of the pure acid solution to lower values of current density indicating the inhibition of both hydrogen evolution (HER) and Zn dissolution reactions. The corrosion potential ( $E_{corr}$ ), cathodic and anodic Tafel slopes ( $\beta_c$  and  $\beta_a$ ), degree of surface coverage ( $\theta$ ) and percentage inhibition efficiency (% IE) were derived from the curves of Fig. 5, and recorded in Table 4. It is evident that by increasing the inhibitor concentration a decrease in corrosion current densities and an increase in inhibition percentage were observed, suggesting that the adsorption protective film tends to be more complete and stable on zinc surface and hence inhibition occurs. Thus, addition of the inhibitor hindered acid attack on the zinc electrode. The maximum inhibition efficiency (85.2%) was reached at an optimum concentration of  $5 \times 10^{-5}$  M of compound (a). A compound can be classified as a cathodic or an anodic type inhibitor when the change in  $E_{corr}$  value is at least 85 mV in relation to that one measured for the blank solution.<sup>31</sup> However, a shift of corrosion potential of compound (a) is about 19 mV and for compound (b) is 33 mV. Therefore, compounds (a and b) might act as a mixed-type inhibitor without changing the mechanism of hydrogen evolution of zinc dissolution. The order of decreasing inhibition efficiency of the investigated chromones is as follows: a > b.

#### Electrochemical Impedance Spectroscopy

The corrosion behavior of zinc in 0.5 M  $\text{H}_2\text{SO}_4$  in the absence and presence of different concentrations of chromones

**Table 4.** The effect of concentration of the investigated chromones on the free corrosion potential ( $E_{corr}$ ), corrosion current density ( $i_{corr}$ ), Tafel slopes ( $\beta_a$  &  $\beta_c$ ), inhibition efficiency (% IE), and degree of surface coverage ( $\theta$ ) for the corrosion of zinc in 0.5 M  $\text{H}_2\text{SO}_4$  at 25 °C

Compound	Conc, M	$-E_{corr}$ , mV vs SCE	$i_{corr}$ , mA cm <sup>-2</sup>	$\beta_c$ , mV dec <sup>-1</sup>	$\beta_a$ , mV dec <sup>-1</sup>	$\theta$	% IE
(a)	0.5 M $\text{H}_2\text{SO}_4$	941	41.2	792	911	—	—
	$1 \times 10^{-6}$	964	22.1	781	895	0.464	46.4
	$3 \times 10^{-6}$	962	12.7	774	886	0.692	69.2
	$5 \times 10^{-6}$	958	8.97	770	879	0.782	78.2
	$1 \times 10^{-5}$	945	8.03	766	871	0.805	80.5
	$3 \times 10^{-5}$	957	7.24	738	868	0.824	82.4
	$5 \times 10^{-5}$	958	6.11	731	862	0.852	85.2
(b)	$1 \times 10^{-6}$	930	25.1	788	902	0.391	39.1
	$3 \times 10^{-6}$	946	15.7	779	891	0.619	61.9
	$5 \times 10^{-6}$	955	11.6	776	887	0.718	71.8
	$1 \times 10^{-5}$	953	9.3	772	879	0.774	77.4
	$3 \times 10^{-5}$	957	8.5	754	872	0.793	79.3
	$5 \times 10^{-5}$	963	7.8	748	868	0.811	81.1

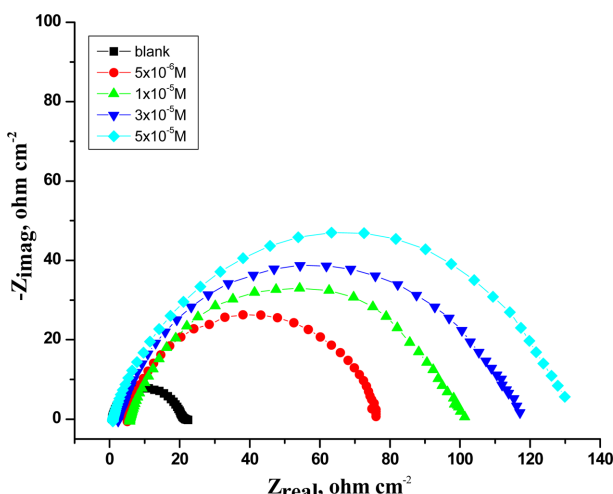


**Figure 6.** Nyquist plots for corrosion of zinc in 0.5 M  $\text{H}_2\text{SO}_4$  in the absence and presence of different concentrations of compound (a) at 25 °C.

was investigated by the EIS method at 25 °C. Fig. 6 shows the Nyquist plots for zinc in 0.5 M  $\text{H}_2\text{SO}_4$  solution in the absence and presence of different concentrations of compound (a). Similar curves were obtained for other chromones (b) (not shown). In 0.5 M  $\text{H}_2\text{SO}_4$  solution and in the presence of various concentrations of inhibitors, the impedance diagrams show the same trend (one capacitive loop), however the diameter of this capacitive loop increases with increasing the inhibitor concentration, due to the increase in the number of adsorbed inhibitor molecules when the

concentration was raised. The fact that impedance diagrams have an approximately semicircular appearance shows that the corrosion of zinc is controlled by a charge transfer process. Small distortion was observed in some diagrams, this distortion has been attributed to frequency dispersion.<sup>32</sup> The equivalent circuit that describes our metal/electrolyte interface is shown in Fig. 7 where  $R_s$ ,  $R_{ct}$  and  $C_{dl}$  refer to solution resistance, charge transfer resistance and double layer capacitance, respectively. The surface coverage ( $\theta$ ) and the inhibition efficiencies (% IE) were calculated from Eq. (4). The associated parameters with the impedance diagrams are given in Table 5. From the impedance results Table 5, we found that as the inhibitor concentration increased,  $R_{ct}$  values increased, but  $C_{dl}$  values tended to decrease. The decrease in  $C_{dl}$  at the metal/solution interface with increasing the inhibitor concentration results from a decrease in local dielectric constant and/or an increase in the thickness of the electrical double layer, suggests that chromone derivatives function by adsorption at the metal/electrolyte interface.<sup>33</sup> The increase in  $R_{ct}$  values was caused by the gradual replacement of water molecules by the adsorption of the inhibitor molecules on the metal surface to form an adherent film reducing the extent of dissolution.<sup>34</sup> The order of inhibition efficiency obtained from EIS measurements decreases as follows: a > b.

#### Electrochemical Frequency Modulation Measurements (EFM)

The EFM is a non destructive corrosion measurement technique that can directly give values of the corrosion current without prior knowledge of Tafel constants. The theory of EFM technique is previously reported.<sup>35,36</sup> Fig. 8 shows the intermodulation spectra obtained from EFM measurements of zinc in 0.5 M  $\text{H}_2\text{SO}_4$  solution in the absence and presence of different concentrations of the investigated compound (a). Similar curves were obtained for the other chromones (b) (not shown). The calculated corro-

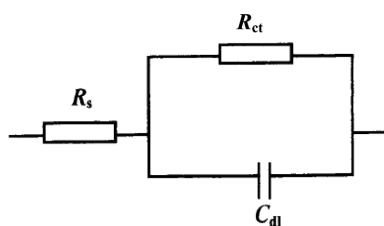


**Figure 7.** Equivalent circuit model used to fit the impedance spectra.

**Table 5.** Electrochemical kinetic parameter obtained by EIS technique for the corrosion of zinc in 0.5 M  $\text{H}_2\text{SO}_4$  in the absence and presence of different concentrations of the investigated chromones at 25°C

Compound	Conc., M	$C_{dl}$ , $\mu\text{F cm}^{-2}$	$R_{ct}$ , $\text{ohm cm}^2$	$\theta$	% IE
blank	0.5 M $\text{H}_2\text{SO}_4$	796.3	22.1	–	–
(a)	$5 \times 10^{-6}$	253.6	72.5	0.695	69.5
	$1 \times 10^{-5}$	143.3	96.7	0.771	77.1
	$3 \times 10^{-5}$	97.6	118.4	0.813	81.3
	$5 \times 10^{-5}$	73.7	134.2	0.835	83.5
	$5 \times 10^{-6}$	341	59.2	0.626	62.6
(b)	$1 \times 10^{-5}$	214	74.2	0.702	70.2
	$3 \times 10^{-5}$	142	86.8	0.745	74.5
	$5 \times 10^{-5}$	109	108	0.795	79.5

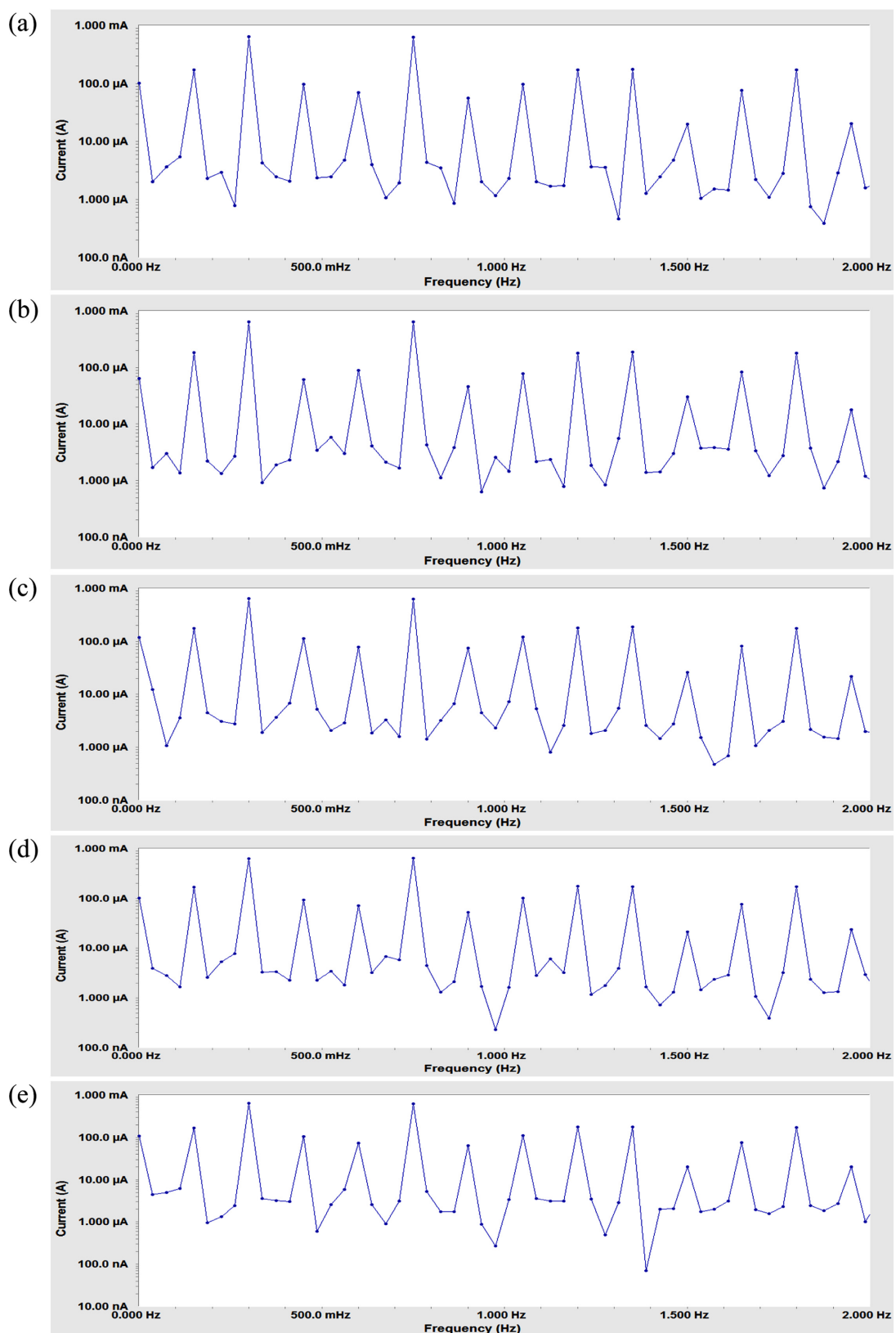


**Figure 8.** Intermodulation spectra for corrosion of zinc in 0.5 M  $\text{H}_2\text{SO}_4$  alone (a) and with  $5 \times 10^{-6} \text{ M}$  (b),  $1 \times 10^{-5} \text{ M}$  (c),  $3 \times 10^{-5} \text{ M}$  (d) and  $5 \times 10^{-5} \text{ M}$  (e) of compound (a).

**Table 6.** Electrochemical parameters obtained by EFM technique for the corrosion of zinc in 0.5 M H<sub>2</sub>SO<sub>4</sub> in the absence and presence of different concentrations of the investigated chromones at 25 °C

Comp.	Conc., M	i <sub>corr</sub> μA cm <sup>-2</sup>	β <sub>a</sub> , mV dec <sup>-1</sup>	-β <sub>c</sub> , mV dec <sup>-1</sup>	CF-2	CF-3	θ	% IE
blank	0.5 M H <sub>2</sub> SO <sub>4</sub>	369	80	181	1.83	2.91	—	—
(a)	5×10 <sup>-6</sup>	153	89	131	1.85	2.88	0.585	58.5
	1×10 <sup>-5</sup>	118	93	144	1.75	3.08	0.680	68.0
	3×10 <sup>-5</sup>	85	96	150	1.89	2.93	0.769	76.9
	5×10 <sup>-5</sup>	56	101	166	1.87	3.10	0.848	84.8
(b)	5×10 <sup>-6</sup>	179	89	136	1.964	2.876	0.515	51.5
	1×10 <sup>-5</sup>	141	88	124	1.853	2.893	0.618	61.8
	3×10 <sup>-5</sup>	109	86	123	1.790	2.713	0.704	70.4
	5×10 <sup>-5</sup>	78	82	117	1.874	2.889	0.788	78.8

sion kinetic parameters at different concentrations of the chromones in 0.5 M H<sub>2</sub>SO<sub>4</sub> at 25 °C (*i*<sub>corr</sub>, β<sub>a</sub>, β<sub>c</sub>, CF-2, CF-3 and %IE) is given in *Table 6*. From this Table, the corrosion current densities decrease and the inhibition efficiencies increase by increasing the concentration of investigated chromones. The great strength of the EFM is the causality factor, which serves as an internal check on the validity of the EFM measurement.<sup>37</sup> Values of causality factors in *Table 6* indicate that the measured data are of good quality. The standard values for CF-2 and CF-3 are 2.0 and 3.0, respectively. The deviation of causality factors from their ideal values might due to that the perturbation amplitude was too small or that the resolution of the frequency spectrum is not high enough. The order of inhibition efficiency obtained from EFM measurements decreases as follows: a > b.

The results obtained from EFM showed good agreement with the obtained from weight loss, polarization and EIS methods.

### Mechanism of Inhibition

Corrosion inhibition of zinc in 0.5 M H<sub>2</sub>SO<sub>4</sub> solution by the investigated chromones as indicated from chemical and electrochemical techniques was found to depend on the concentration and the nature of the inhibitors. It is generally assumed that adsorption of the inhibitor at the metal/solution interface is the first step in the action mechanism of the inhibitors in aggressive acid media. Four types of adsorption may take place during inhibition involving organic molecules at the metal / solution interface:<sup>38</sup>

i) Electrostatic attraction between charged molecules and charged metal ii) Interaction of unshared electrons pairs in the molecule with the metal iii) Interaction of π electrons with the metal and iv) A combination of the above. Concerning inhibitors, the inhibition efficiency depends on several factors; such as: (a) the number of adsorption sites and their charge density, (b) molecular size, heat of

hydrogenation, (c) mode of interaction with the metal surface, and (d) the formation metallic complexes.<sup>39</sup>

Most organic inhibitors contain at least one polar group with an atom of nitrogen, sulfur or oxygen, each of them in principle representing an adsorption center. The inhibitive properties of such inhibitors depend on the electron densities surrounding the adsorption centers: the higher the electron density at the center, the more the effective the inhibitor. Also, it is apparent that the adsorption of these inhibitor molecules on the zinc surface could occur directly on the basis of donor-acceptor behavior between the lone pairs of the heteroatom and the extensively delocalized π-electrons of the inhibitor molecule and the vacant d-orbital of zinc surface atoms.<sup>40</sup> These inhibitors are able to absorb on anodic sites through O atoms, heterocyclic and aromatic rings which are electron donating groups. The adsorption of these inhibitors on anodic sites may decrease anodic dissolution of zinc. In the aqueous acidic solutions, most of organic inhibitors exist either as neutral molecules or in the form of cations (protonated). In general two modes of adsorption could be considered. In our case, since Zn surface acquires negative charge in acidic solutions<sup>41,42</sup> and the investigated compounds are protonated in acidic media (acquire positive charge) the inhibitor molecules may adsorb on the zinc surface via the physisorption mechanism, involving the displacement of water molecules from the metal surface and the sharing electrons between the O atoms and zinc.

The order of increased inhibition efficiency for chromones is: a > b as indicated from the different methods. Inhibitor (a) is more efficient inhibitor due to its larger molecular size and the presence of three OCH<sub>3</sub> groups which have higher electron donation character. On the other hand, inhibitor (b) is less effective inhibitor due to its lower molecular size and the presence of Br atom which has electron withdrawing character.

## CONCLUSIONS

The investigated chromones are good inhibitors for zinc corrosion in 0.5 M H<sub>2</sub>SO<sub>4</sub>. The potentiodynamic polarization data indicated that chromones are mixed type inhibitors and are adsorbed on Zn surface obeying Langmuir adsorption isotherm. The EIS measurements suggest that chromones inhibit the zinc dissolution by adsorption at metal surface thereby causing the decrease in  $C_{dl}$  values and increasing in  $R_{ct}$  values. The results obtained from weight loss, polarization, EIS and EFM studies are in good agreement.

**Acknowledgments.** Publication cost of this paper was supported by the Korean Chemical Society.

## REFERENCES

1. Singh, A. K. *Ind. Eng. Chem. Res.* **2012**, *51*, 3215.
2. Singh, A. K.; Quraishi, M. A.; Ebenso, E. E. *Int. J. Electrochem. Sci.* **2011**, *6*, 5676.
3. Nazeer, A. A.; El-Abbasy, H. M.; Fouda, A. S. *Res. Chem. Intermed.* **2013**, *39*, 921.
4. Singh, V. P.; Singh, P.; Singh, A. K. *Inorg. Chim. Acta* **2011**, *379*, 56.
5. Nazeer, A. A.; El-Abbasy, H. M.; Fouda, A. S. *J. Mater. Eng. Perform.* **2013**, *22*, 2314.
6. Kawai, S.; Kato, H.; Hayakawa, T. *Denki Kagaku Oyobi Kogyo Butsuri Kagaku* **1971**, *39*(4), 28.
7. Grigorev, V. P.; Ekilik, V. V. *Protection of Metals* **1968**, *4*, 1.
8. El-Gaber, A. S.; Fouda, A. S.; El-Desoky, A. M. *Clencia and Technologia des Materiais* **2008**, *20*, 71.
9. Fouda, A. S.; Abdallah, M.; Atwa, S. T.; Salem, M. M. *Modern Appl. Sci.* **2010**, *4*, 41.
10. Shams El-Din, A. M.; El-Hosary, A. A. *Werkst. Korros.* **1977**, *28*(1), 26.
11. Kawai, S.; Kato, H.; Hayakawa, Y. *DEAKI Kagaku* **1971**, *39*(4), 288.
12. Antropov, L. I.; Pogrebova, I. S.; Dremova, G. I. *Zashch. Met.* **1971**, *7*(1), 3.
13. Wang, L.; Pu, J. X.; Luo, H. C. *Corros. Sci.* **2003**, *45*(4), 677.
14. Agrawal, Y. K.; Talati, J. D.; Shah, M. D.; Desai, M. N.; Shah, N. K. *Corros. Sci.* **2004**, *46*(3), 633.
15. Talati, J. D.; Desai, M. N.; Shah, N. K. *Mater. Chem. Phys.* **2005**, *93*(1), 54.
16. Subramanyam, N.; Ramakrishnaiah, K. *Indian J. Technol.* **1970**, *8*, 369.
17. Pharma, S.; Gaur, I. N. *Electrochem. Soc. India* **1976**, *25*(A), 138.
18. Abdel Aal, M. S.; Abdel Wahab, A. A.; El-Saied, A. *Corrosion* **1981**, *37*(10), 557.
19. Kuzntnov, V. A.; Loaf, Z. A. *J. Phys. Chem. (U.S.S.R.)* **1957**, *21*, 201.
20. Bentiss, F.; Lebrini, M.; Lagrenée, M. *Corros. Sci.* **2005**, *47*, 915.
21. Szklarska-Smialowska, Z. *Electrochemical and Optical Techniques for the Study of Metallic Corrosion*; Kluwer Academic: the Netherlands, 1991; pp 545.
22. Langmuir, I. *J. Amer. Chem. Soc.* **1947**, *39*, 1848.
23. Khamis, E. *Corrosion* **1990**, *46*, 476.
24. Popova, A.; Sokolova, E.; Raicheva, S.; Chritov, M. *Corros. Sci.* **2003**, *45*, 33.
25. Szklarska-Smialowska, Z.; Mankovwski, J. *Corros. Sci.* **1978**, *18*, 953.
26. Yurt, A.; Ulutas, S.; Dal, H. *Appl. Surf. Sci.* **2006**, *253*, 919.
27. Zarrok, H.; Salghi, R.; Zarrouk, A.; Hammouti, B.; Oudda, H.; Bazzi, Lh.; Bammou, L.; Al-Deyab, S. S. *Der Pharma Chemica* **2012**, *4*(1), 407.
28. Dahmani, M.; Al-Deyab, S. S.; Et-Touhami, A.; Hammouti, B.; Bouyanzer, A.; Salghi, R.; ElMejdoubi, A. *Int. J. Electrochem. Sci.* **2012**, *7*, 2513.
29. Martinez, S.; Stern, I. *Appl. Surf. Sci.* **2002**, *199*, 83.
30. Singh, G.; Jha, L.; Verkey, D. *Trans. SAEST* **1990**, *25*, 29.
31. Li, W.; He, Q.; Zhang, S.; Pei, C.; Hou, B. *J. Appl. Electrochem.* **2008**, *38*, 289.
32. Mansfeld, F.; Kendig, M. W.; Tsai, S. *Corrosion* **1982**, *38*, 570.
33. McCafferty, E.; Hackerman, N. *J. Electrochem. Soc.* **1972**, *119*, 146.
34. Muralidharan, S.; Phani, K. L. N.; Pitchumani, S.; Ravichandran, S. *J. Electrochem. Soc.* **1995**, *42*, 1478.
35. Bosch, R. W.; Hubrecht, J.; Bogaerts, W. F.; Syrett, B. C. *Corrosion* **2001**, *57*, 60.
36. Abdel-Rehim, S. S.; Khaled, K. F.; Abd-Elshafi, N. S. *Electrochim. Acta* **2006**, *51*, 3269.
37. Bentiss, F.; Bouanis, M.; Mernari, B.; Traisnel, M.; Vezin, H.; Lagrenée, M. *Appl. Surf. Sci.* **2007**, *253*, 3696.
38. Schweinsberg, D.; George, G.; Nanayakkara, A.; Steiner, D. *Corros. Sci.* **1988**, *28*, 55.
39. Fouda, A. S.; Mousa, M. N.; Taha, F. I.; Elneanaa, A. I. *Corros. Sci.* **1986**, *26*, 719.
40. Muralidharan, S.; Quraishi, M. A.; Iyer, S. V. K. *Corros. Sci.* **1995**, *37*, 1739.
41. Antropov, L. I. *Corros. Sci.* **1967**, *7*, 607.
42. Abdallah, M.; Atwa, S. T.; Salem, M. M.; Fouda, A. S. *Int. J. Electrochem. Sci.* **2013**, *8*, 10001.